

Article

Not peer-reviewed version

Ice Core ^{17}O Reveals Past Changes in Surface Air Temperatures and Stratosphere to Troposphere Mass Exchange

[Pradeep K Aggarwal](#)*, Frederick J Longstaffe, Franklin W Schwartz

Posted Date: 7 August 2023

doi: 10.20944/preprints202308.0523.v1

Keywords: Isotope; Oxygen-17; Ice Core; Paleothermometry; Stratosphere; Brewer-Dobson Circulation



Preprints.org is a free multidiscipline platform providing preprint service that is dedicated to making early versions of research outputs permanently available and citable. Preprints posted at Preprints.org appear in Web of Science, Crossref, Google Scholar, Scilit, Europe PMC.

Copyright: This is an open access article distributed under the Creative Commons Attribution License which permits unrestricted use, distribution, and reproduction in any medium, provided the original work is properly cited.

Article

Ice Core ^{17}O Reveals Past Changes in Surface Air Temperatures and Stratosphere to Troposphere Mass Exchange

Pradeep K. Aggarwal ^{1,*}, Frederick J. Longstaffe ² and Franklin W. Schwartz ³

¹ International Atomic Energy Agency, Vienna, Austria

² Department of Earth Sciences, The University of Western Ontario, London, Ontario, Canada

³ School of Earth Sciences, The Ohio State University, Columbus, Ohio, USA

* Correspondence: Corresponding author: Pradeep Aggarwal (pkaggarwal@gmail.com)

† now retired from IAEA.

Abstract: In this study, we have investigated the oxygen isotope compositions ($\delta^{17}\text{O}$ and $\delta^{18}\text{O}$) of modern rain and ice cores using published isotopic data. We find that, contrary to existing interpretations, precipitation $\delta^{17}\text{O}$ is influenced by two factors: mass-dependent fractionation (MDF) that occurs during ocean evaporation, and mass-independent fractionation (MIF) that happens in the stratosphere. The MDF contribution remains constant and can be understood from studying tropical rain, as the overall movement of mass in the tropics is upward towards the stratosphere. On the other hand, the MIF effect comes from the mixing of stratospheric air in the troposphere, which is a result of the Brewer-Dobson circulation. This MIF effect on precipitation ^{17}O increases from the tropics towards the poles and is observed consistently in modern precipitation and ice cores. The relative $\delta^{17}\text{O}$ and $\delta^{18}\text{O}$ composition, denoted as $\Delta^{17}\text{O}$, in modern precipitation can be calibrated with surface air temperature, creating a new, independent tool for estimating past temperatures. We used this calibration along with $\Delta^{17}\text{O}$ of Antarctic and Greenland ice cores and our reconstructed past temperatures are in excellent agreement with those from borehole thermometry or gas phase analysis of air trapped in the ice. The $\Delta^{17}\text{O}$ method overcomes the problems associated with using $\delta^{18}\text{O}$ for paleothermometry. Our findings align with climate models that suggest a weakening of the Brewer-Dobson circulation during the Last Glacial Maximum. Furthermore, our method could be used to monitor future changes in stratosphere – troposphere mass exchange in response to a warming climate caused by increasing greenhouse gases.

Keywords: isotope; oxygen-17; ice core; paleothermometry; stratosphere; Brewer-Dobson circulation

1. Introduction

Oxygen and hydrogen isotope compositions ($\delta^{18}\text{O}$ and $\delta^2\text{H}$) in polar ice offer strong evidence of both long-term and abrupt climate changes. Temporal and spatial variations in $\delta^{18}\text{O}$ and $\delta^2\text{H}$ facilitate reconstruction of recurrent climate changes in past glacial and interglacial cycles (Dansgaard et al., 1993; Johnsen et al., 2001; Petit et al., 1999). The use of isotopes to derive climatic information has focused on the quantification of surface air temperatures and changes in the hydrological cycle (Schmidt et al., 2007; Jouzel et al., 2013). However, the $d^{18}\text{O}$ – temperature relationship (d/T slope) cannot be calibrated and yields different results when evaluated for spatial or temporal (e.g., ice core at different depths) variations (Jouzel et al., 1997; 2003). In coastal Antarctica, variations in surface temperature do not appear to influence the $d^{18}\text{O}$ of shallow ice cores (Goursaud et al., 2019). The estimates of Antarctic or Greenland temperature changes from the Last Glacial Maximum (LGM, ~29 – 19 kyr before present) to Holocene (~11.7 kyr to present), or during abrupt events in Greenland, derived from ice core $d^{18}\text{O}$ are much different than those derived from borehole thermometry (Cuffey et al., 1995, 2016) or gas phase analysis that uses models of firn densification and thermal fractionation

of gases analyzed from trapped air in the ice (Severinghaus and Brook, 1999). The $d^{18}\text{O}$ based estimates of past temperature increase from the LGM to Holocene is smaller by 10 – 16 °C compared to those based on borehole or gas phase analysis thermometry. Similarly, the magnitude of cooling or warming during abrupt climate change events is smaller when estimated from $\delta^{18}\text{O}$ compared to that from trapped air in ice. Borehole thermometry is not applicable for quantifying abrupt temperature changes (Cuffey et al., 1995; Jouzel et al., 1997; 2003) and gas phase analysis of trapped air may be less reliable in regions of low snow accumulation such as East Antarctica (Jouzel et al., 2003). Gas phase analysis can also yield conflicting temperature estimates because of differences in models of heat and ice flow and firn densification. For example, at the NGRIP ice core site in Greenland, differing LGM temperatures or warming trends during deglaciation have been indicated based on the same dataset of gas phase compositions (Buizert et al., 2014; Kindler et al., 2014).

Hydrological cycle changes inferred from isotopic data have included sea surface temperature and relative humidity in oceanic moisture source regions and the amount of precipitation or accumulation in polar areas (Schmidt et al., 2007; Jouzel et al., 2013). Precipitation isotope variability is also weakly correlated with large-scale hemispherical modes (southern and northern annular modes) of circulation (Schmidt et al., 2007) that are connected with the stratosphere through changes in the strength of the polar vortices (Thompson and Solomon, 2003; Baldwin et al., 2019). However, precipitation $d^{18}\text{O}$ and $d^2\text{H}$ contents in precipitation are not useful for characterizing changes in stratosphere – troposphere interactions (Schmidt et al., 2005).

More recently, small but significant variations have been observed in the relative composition of precipitation $d^{17}\text{O}$ versus $d^{18}\text{O}$. These differences have been interpreted to reflect a variable mass-dependent fractionation (MDF) owing to variable relative humidity during ocean evaporation in the moisture source region (Angert et al., 2004; Luz and Barkan, 2010; Landais et al., 2008; Uemura et al., 2010). This framework, however, does not adequately explain ^{17}O variations in polar precipitation and ice cores (Miller and Pack, 2021; Steig et al., 2021), leading to the suggestion that, in natural waters, MDF is associated with different coefficients from the tropics to the poles (Sharp et al., 2018).

Commonly, interpretations of ^{17}O levels in natural waters do not account for contributions from stratosphere-sourced ^{17}O (Sharp et al., 2018; Steig et al., 2020; Miller and Pack, 2021). Mass-independent fractionations (MIF) during ozone photolysis reactions in the stratosphere produce much higher $d^{17}\text{O}$ relative to $d^{18}\text{O}$, compared to $d^{17}\text{O} \approx 0.5 d^{18}\text{O}$ resulting from MDF (Thiemens, 2006). Although a stratospheric ^{17}O input has been suggested for the Antarctic (Winkler et al., 2013; Pang et al., 2022) and Arctic (Lin et al., 2013) snow, it is not considered as a ubiquitous source contributing normally to global precipitation. In contrast, a stratospheric input is known to influence the ^{17}O contents of tropospheric gases (ozone, molecular oxygen and carbon dioxide) or nitrate and sulfate aerosols (Thiemens, 2006).

Here, we investigate the roles of MDF and stratospheric input in determining the $d^{17}\text{O}$ of precipitation by using the $d^{17}\text{O}$ and $d^{18}\text{O}$ values of tropical to polar precipitation and ice cores from the published literature. We then explore the relative difference between $d^{17}\text{O}$ and $d^{18}\text{O}$ compositions ($D^{17}\text{O}$) as an independent paleothermometer based on an empirical calibration of with temperature data for modern precipitation. Our approach is based on the hypothesis that the magnitude of $D^{17}\text{O}$ is affected by stratospheric input when precipitation forms, but is unaffected by subsequent water cycle processes because those processes would all involve a mass-dependent fractionation of ^{17}O and ^{18}O that does not change $D^{17}\text{O}$. Our results show that the $D^{17}\text{O}$ of precipitation and ice cores provides a robust tool for monitoring stratosphere to troposphere mass exchange. The $D^{17}\text{O}$ paleothermometer is more robust compared to that based on a single isotope ($d^{18}\text{O}$) and inherently compensates for the effects of seasonality or altitude of precipitation and different seawater $d^{18}\text{O}$ compositions in the past.

2. Stratospheric Input and Precipitation ^{17}O

2.1. Mass-dependent fractionation coefficient

Detailed descriptions and reviews of current knowledge concerning ^{17}O distribution in natural waters are available in the published literature (Angert et al., 2004; Luz and Barkan, 2010; Landais et al., 2008; Uemura et al., 2010; Steig et al., 2021; Miller and Pack, 2021; Sharp et al., 2018; Thiemens, 2006; Aron et al., 2021). Briefly, mass-dependent, kinetic or equilibrium isotopic fractionation (MDF) of oxygen isotopes in water cycle processes, such as evaporation, diffusion, and condensation, is expressed using the conventional d notation as follows:

$$\ln(1 + d^{17}\text{O}/1000) = l \ln(1 + d^{18}\text{O}/1000) \quad (1)$$

where $d = 10^3 (R_{\text{sample}}/R_{\text{standard}} - 1)$, R is the isotope ratio ($^{17}\text{O}/^{16}\text{O}$ or $^{18}\text{O}/^{16}\text{O}$) in a sample or the VSMOW isotopic standard, and l is a constant for mass-dependent fractionation (MDF coefficient). In the commonly used notation for triple isotope systems, Eq. 1 is written as:

$$d^{17}\text{O} = l d^{18}\text{O} \quad (2)$$

The d' values are slightly more negative than the d values, but are used for triple isotope evaluations so that the $d^{17}\text{O} - d^{18}\text{O}$ relationship becomes linear (Miller and Pack, 2021). Deviations from mass-dependent fractionation are given as (Miller and Pack, 2021):

$$\Delta^{17}\text{O} \text{ (per meg or ppm)} = 10^3 (d^{17}\text{O} - l d^{18}\text{O}) \quad (3)$$

The MDF coefficient (l) has a value of approximately 0.5 (Miller and Pack, 2021). For natural waters, the actual fractionation processes are not easily quantified and therefore the l value is determined empirically (Eq. 2) as the regression slope of $d^{17}\text{O}$ versus $d^{18}\text{O}$ (Miller and Pack, 2021). This regression is conducted using a diverse set of natural water samples and it is assumed that the ^{17}O of those samples is affected only by mass-dependent isotope fractionation. A l value of 0.528 was determined (Meijer and Li, 1998; Luz and Barkan, 2010) by using isotopic data from water samples of precipitation, lakes, rivers, springs, and ice cores collected from the tropics to Antarctica. The resulting $\Delta^{17}\text{O}$ values are quite variable, with a positive or negative slope in the $\Delta^{17}\text{O} - d^{18}\text{O}$ space, and are mostly greater than zero (Figure 1). The $\Delta^{17}\text{O}$ values are less than zero for a smaller proportion of ice core and extratropical precipitation samples (Figure 1).

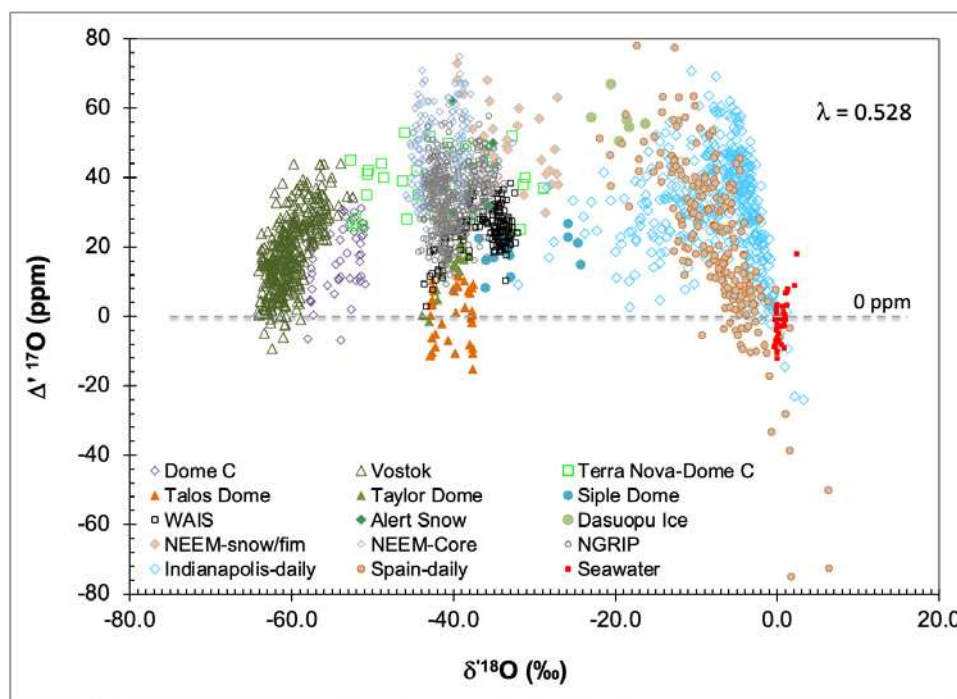


Figure 1. $\Delta^{17}\text{O}$ for precipitation and ice cores using a MDF coefficient of 0.528. Note the variable $\Delta^{17}\text{O}$ versus $d^{18}\text{O}$ correlation at low and high $d^{18}\text{O}$ values.

Mass-dependent fractionation processes, by definition, result in $\Delta^{17}\text{O}$ values of zero (Thiemens, 2006). Therefore, the positive or negative $\Delta^{17}\text{O}$ values in natural waters have been attributed to

different MDFs in equilibrium ($\text{MDF I} = 0.529$) and kinetic ($\text{MDF I} = 0.519$) fractionation processes. The proportions of equilibrium or kinetic MDF are considered to vary depending upon the relative humidity during ocean evaporation in the moisture source region (Uemura et al., 2010; Landais et al., 2008). This $\text{D}'^{17}\text{O}$ behavior is analogous to that of relative d^{18}O and d^2H composition (d-excess), which is also interpreted to reflect humidity and/or sea surface temperature variations in the moisture source region. However, $\text{D}'^{17}\text{O}$ and d-excess in ice cores are not well correlated (Steig et al., 2021; Miller and Pack, 2021). The ocean relative humidity during the LGM based on d^{17}O of ice cores is inferred to be higher compared to present-day values. This finding appears to be inconsistent with recent observational trends or climate model predictions (Sherwood et al., 2009). Following several studies with extensive isotopic datasets, the humidity dependence of MDF in the moisture source region is insufficient to explain the observed $\text{D}'^{17}\text{O}$ variations in precipitation and ice cores (Steig et al., 2021; Miller and Pack, 2021).

An alternative is that the MDF coefficient in water cycle processes may simply be variable in polar and non-polar precipitation instead of a constant value of 0.528 (Sharp et al., 2018). There is, however, no predictive mechanism available for quantifying the geographical or climatic variations for this MDF coefficient. Consequently, the causes of $\text{D}'^{17}\text{O}$ variability in modern or past precipitation remain poorly understood (Steig et al., 2021; Miller and Pack, 2021, Sherwood et al., 2009).

This lack of understanding of $\text{D}'^{17}\text{O}$ variations could also be a consequence of an incomplete representation of processes affecting natural water ^{17}O levels in the presently accepted MDF coefficient of 0.528. As noted above, this coefficient was estimated from a dataset that included samples of Antarctic ice (Luz and Barkan, 2010; Landais et al., 2008), which has been shown to contain a stratospheric input (Winkler et al., 2014; Pang et al., 2022). Similarly, upper tropospheric moisture contributing to extratropical precipitation may also include a MIF component because of stratosphere to troposphere transport that occurs mostly at high latitudes (Holton et al., 1995). Indeed, a lower MDF coefficient of 0.525 is obtained when Antarctic and mid- to high-latitude samples are excluded from the presently used reference dataset of Luz and Barkan (2010). This is lowered further to 0.523, when lakes and ponds also are excluded as d^{17}O in some of these samples was considered to have been affected by evaporation (Luz and Barkan, 2010). Therefore, the existing evidence indicates that the influence of stratospheric input of ^{17}O on precipitation ^{17}O must be evaluated in order to characterize the MDF coefficient.

Stratospheric air, including water vapor, reaches the troposphere by stratosphere to troposphere transport (STT) driven by the meridional Brewer-Dobson Circulation (BDC) (Holton et al., 1995; Rosenlof, 1995). The BDC acts as an “extratropical pump” (Figure S1) with upwelling of tropospheric air across the tropopause in the tropics ($23^\circ\text{N} - 23^\circ\text{S}$ latitude), poleward transport within the stratosphere, and downwelling of stratospheric air at high latitudes (poleward of $\sim 60^\circ\text{N}$ or $\sim 50^\circ\text{S}$) of the winter hemisphere (Holton et al., 1995; Rosenlof, 1995). Tropospheric moisture in the tropics is derived mostly from ocean evaporation (Figures S1 and S2) and the water vapor mixing ratio decreases with altitude to ~ 10 ppmv near the tropopause ($\sim 10\text{--}18$ km) (Holton et al., 1995; Sherwood et al., 2009). This air is further dehydrated to a mixing ratio of $\sim 2\text{--}3$ ppmv by freeze-drying across the tropopause before entering the stratosphere (Holton et al., 1995), with its d^{17}O reflecting mass-dependent fractionation ($\text{d}^{17}\text{O} \approx 0.5 \text{ d}^{18}\text{O}$) in ocean evaporation (Franz and Rockmann, 2005; Brinjkiji and Lyons, 2021). In the stratosphere, water vapor d^{17}O increases by isotope exchange with NO_x species, which have a higher ^{17}O abundance as a result of MIF (Thiemens, 2006; Franz and Rockmann, 2005; Brinjkiji and Lyons, 2021; Zahn et al., 2006). The water vapor mixing ratio of stratospheric air nearly doubles to $\sim 4\text{--}6$ ppmv (Holton et al., 1995) due to *in situ* production by methane oxidation. This *in situ* production occurs with oxygen that carries an MIF imprint resulting in water vapor that has higher d^{17}O compared to that from MDF (Franz and Rockmann, 2005; Brinjkiji and Lyons, 2021; Zahn et al., 2006). Stratospheric water vapor with elevated d^{17}O reaches the troposphere in the downward flow of the BDC at high latitudes. Higher $\text{d}^{17}\text{O}/\text{d}^{18}\text{O}$ ratios (with $\text{D}'^{17}\text{O}$ values of ~ -2000 ppm) have been observed in upper tropospheric moisture just below the tropopause poleward of $\sim 64^\circ\text{S}$ latitude (Franz and Rockmann, 2005). As the net vertical transport of water vapor in the tropics

is towards the stratosphere (Franz and Rockmann, 2005), the latitudinal variability in STT would also result in a variable $d^{17}\text{O}/d^{18}\text{O}$ ratios (or $D^{17}\text{O}$) of the upper tropospheric moisture.

Upper tropospheric moisture in turn is incorporated in precipitation (Matejka et al., 1980; Houze, 2014). This is indicated also by the ubiquitous presence of cosmogenic tritium that is produced predominantly in the stratosphere and is also carried to the troposphere by STT (Lal and Peters, 1967; Fourre et al., 2018). Latitudinal variability in $d^{17}\text{O}/d^{18}\text{O}$ ratios (or $D^{17}\text{O}$) of upper tropospheric moisture therefore can be reflected in precipitation. An inverse correlation of tritium and $d^{18}\text{O}$ is observed in Antarctic surface snow (Figure S3). It suggests that a tropospheric moisture component influenced by STT may contribute to the lower $d^{18}\text{O}$ of Antarctic precipitation (Winkler et al., 2013). In non-polar regions, stratiform-type precipitation, which originates largely from tropospheric moisture (Matejka et al., 1980; Houze, 2014), has lower $d^{18}\text{O}$ compared to convective-type precipitation (Aggarwal et al., 2016), which originates largely from moisture in the planetary boundary layer (Matejka et al., 1980; Houze, 2014). Consequently, the $d^{17}\text{O}$ of precipitation may also include a variable component of stratospheric input.

Once precipitation is formed, however, subsequent fractionation in water cycle processes (for example evaporation, sublimation, diffusion, or isotopic exchange in surface snow) would all be mass-dependent with a change in $d^{17}\text{O} \approx 0.5 d^{18}\text{O}$ (Franz and Rockmann, 2005). In other words, if precipitation at different latitudes or in different seasons forms with a tropospheric moisture component which has variable $d^{17}\text{O}/d^{18}\text{O}$ ratios, this variability in isotopic ratios (or $D^{17}\text{O}$) would be preserved because any subsequent isotopic fractionation would be mass-dependent and change the $d^{17}\text{O}$ value by approximately half that of $d^{18}\text{O}$. Indeed, high latitude precipitation poleward of 60°N or 60°S has a $d^{17}\text{O}$ versus $d^{18}\text{O}$ regression slope of 0.529, compared to a slope of 0.527 at lower latitudes towards the equator (Sharp et al., 2018; Aron et al., 2021).

Stratospheric inputs are minimal in the tropics, where the net vertical mass flux is towards the stratosphere. At mid- to high-latitudes, stratospheric inputs increase owing to the Brewer-Dobson Circulation (Figure S1; Holton et al., 1995). Therefore, we can characterize the coefficient of mass-dependent fractionation by evaluating the $d^{17}\text{O} - d^{18}\text{O}$ relationships in tropical and extratropical precipitation. This approach is similar to that used for identifying a stratospheric component in tropospheric O_2 (Luz et al., 1999).

We compiled the $d^{17}\text{O}$ and $d^{18}\text{O}$ values of 858 samples of precipitation and surface water from the published literature (Kaseke et al., 2018; Bhattacharya et al., 2021; He et al., 2021; Aron et al., 2021; Uechi and Uemera, 2019; Tian and Wang, 2019; Luz and Barkan, 2010; Surma et al., 2019; Voigt et al., 2021). These data were separated into subsets of tropical (about $23^\circ\text{N} - 23^\circ\text{S}$ latitude), sub-tropical (about 23° to 30° N or S) and extratropical (30° to 60° N or S) regions.

The $d^{17}\text{O}$ versus $d^{18}\text{O}$ regression slope for tropical precipitation and surface waters (elevation < 1000 m) is 0.521 (Table 1). Combined regression of tropical and subtropical waters also has a slope of 0.521. That value increases to 0.523 when high elevation (~ 1000 to ~ 4600 m) tropical waters (with low $d^{18}\text{O}$ values) are included in the regression. Conversely, tropical and subtropical waters with higher $d^{18}\text{O}$ values ($> -4\text{‰}$) have a lower slope of 0.516 ($n=133$). Although stratospheric input in the tropics is minimal, some of the deep convective and other precipitation may still be influenced by it. Combined isotope and radar studies of precipitation events in California, USA have suggested that lower $d^{18}\text{O}$ precipitation originates at higher altitudes (Coplen et al., 2008). As noted previously, the $d^{18}\text{O}$ of precipitation has been shown to decrease with an increasing proportion of stratiform-type precipitation (Aggarwal et al., 2016) that originates mostly from tropospheric moisture (Matejka et al., 1980; Houze, 2014). Nearly half of the precipitation in the tropics consists of the stratiform fraction (Houze, 2014). The lower regression slope of 0.516 for higher $d^{18}\text{O}$ samples suggests that some of the tropical water samples with slightly lower $d^{18}\text{O}$ may carry some stratospheric influence.

Table 1. Statistical parameters for the linear regression of $d^{17}\text{O}$ versus $d^{18}\text{O}$ in precipitation and surface water samples from the tropics, subtropics and extratropics. High elevation samples are from altitudes greater than 1000 m.

	R^2	Slope	Std. error	p -value	Intercept	Std. error	p -value
Tropical	0.998	0.521	0.002	<0.01	-0.015	0.011	0.13
Tropical+subtropical	0.998	0.521	0.001	<0.01	-0.012	0.008	0.17
Tropical + high elevation	0.998	0.523	0.001	<0.01	-0.011	0.009	0.32
Tropical+subtropical + high elevation	0.998	0.523	0.001	<0.01	-0.008	0.008	0.48
Extratropical	1.0	0.527	0.000	<0.01	0.027	0.001	<0.01
Tropical+subtropical+high elev.+extratropical	0.999	0.525	0.001	<0.01	-0.004	0.004	0.31
Tropical+subtropical+extratropical ($d^{18}\text{O} < -4\text{‰}$)	0.998	0.528	0.001	<0.01	0.032	0.006	<0.01
Extratropical ($d^{18}\text{O} < -4\text{‰}$)	1.0	0.529	0.001	<0.01	0.045	0.001	<0.01
Tropical ($d^{18}\text{O} > -4\text{‰}$)	0.998	0.516	0.003	<0.01	-0.001	0.011	0.93
Extratropical($d^{18}\text{O} > -4\text{‰}$)	1.0	0.520	0.001	<0.01	0.001	0.002	0.52
Tropical+subtropical ($d^{18}\text{O} > -4\text{‰}$)	0.999	0.516	0.002	<0.01	-0.002	0.008	0.80
Tropical+subtropical+extratropical ($d^{18}\text{O} > -4\text{‰}$)	0.999	0.516	0.001	<0.01	-0.003	0.004	0.43

Regression of data from extratropical precipitation alone or together with tropical and subtropical waters gives higher slopes of 0.525 to 0.527 (Table 1). These higher slopes are consistent with a greater influence of stratospheric input in extratropical regions compared to the tropics. Regression of the subset of extratropical precipitation samples with $d^{18}\text{O} > -4\text{‰}$ again results in a lower slope (~ 0.520) compared to that (0.529) for samples with $d^{18}\text{O} < -4\text{‰}$. A combined regression of all samples in our dataset with higher $d^{18}\text{O} (> -4\text{‰})$, including those from the extratropics, results in a regression slope of 0.516 as was noted above for samples only from the tropics (Table 1).

The regression intercepts for all subsets, except when the dataset included all or low- $d^{18}\text{O} (< -4\text{‰})$ extratropical precipitation, are statistically insignificant with p -values of 0.13 to 0.93 (Table 1). Thus, the $d^{17}\text{O}$ versus $d^{18}\text{O}$ regression line for tropical precipitation passes through the origin and indicates that water vapor from ocean evaporation does not have an anomalous ^{17}O compared to that expected from MDF, contrary to the conclusions from previous studies (Landais et al., 2008; Luz and Barkan, 2010).

The 0.516 value for the regression slope of heavier $d^{18}\text{O}$ waters ($> -4\text{‰}$) is nearly the same as the MDF coefficients in other terrestrial processes, including diffusion in air (Barkan and Luz, 2007), plant photosynthesis (Landais et al., 2007), and leaf water evaporation (Landais et al., 2006). It is likely therefore that for natural waters also the MDF coefficient has a value of ~ 0.516 . This value is not substantially different than the 0.521 value obtained from the regression of tropical precipitation excluding high elevations samples (Table 1). In the discussion below, we use 0.516 as the MDF coefficient to evaluate stratospheric input and MDF influence on natural waters. This discussion remains essentially the same if a value of 0.521 is used and we have included the corresponding figures in Supporting Information.

2.2. Influence of stratospheric input on $D^{17}O$

The influence of stratospheric ^{17}O input on precipitation $D^{17}O$ can be evaluated by examining its variability in ice cores, seawater and extratropical precipitation with respect to mass-dependent fractionation in tropical precipitation. As Figure 1 shows, the MDF coefficient value of 0.528 results in variable $D^{17}O - d^{18}O$ correlations for polar snow and ice cores, tropical glaciers, seawater and extratropical precipitation. The same data show a strong correlation with a coefficient value of 0.516 (Figure 2), or 0.521 (Figure S4). The distribution of all of the Antarctic and Arctic snow or ice core samples is defined by a single regression line ($R^2 = 0.996$). Extratropical precipitation with $d^{18}O < -4\text{‰}$ and ice cores from tropical glaciers (Dasuopu) also lie along this trend (Figure 2A). We note that extratropical precipitation with unusually low $d^{18}O$ (~ -31 to -28‰) has nearly the same $D^{17}O$ as Greenland surface snow in a comparable $d^{18}O$ range (Figure 2A). Low $d^{18}O$ in extratropical precipitation commonly occurs during extreme weather conditions with a polar vortex and subsidence of drier, upper tropospheric air (Goering et al., 2001), which would cause $D^{17}O$ values to be similar to polar precipitation.

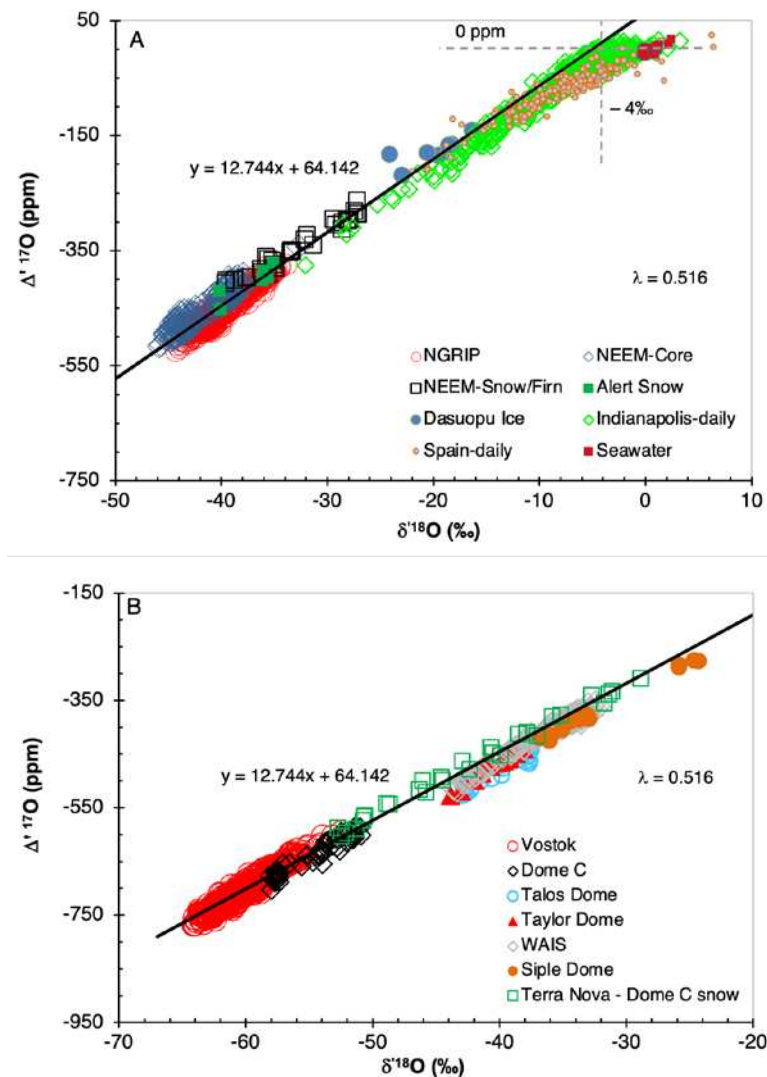


Figure 2. Correlation of $D^{17}O$ and $d^{18}O$ in natural waters. MDF coefficient (λ) value is 0.516. Solid black line in A and B is based on a regression *only* of ice core and snow sample data from the Antarctic and Greenland. **A:** Greenland (NEEM, NGRIP) ice core and snow; Alert (Arctic) snow; Dasuopu (tropical) ice core; extratropical precipitation (Indianapolis, USA and Madrid, Spain). Dashed, gray horizontal and vertical lines highlight specific y and x axis values. **B:** Antarctic ice cores (Vostok,

Dome C, Talos Dome, Taylor Dome; WAIS Divide; Siple Dome) and surface snow (from Terra Nova Bay, upper right corner, to Dome C, lower left).

Seawater and extratropical precipitation with $d^{18}\text{O}$ greater than about -4‰ do not follow the $D^{17}\text{O} - d^{18}\text{O}$ correlation trend defined by polar snow and ice (Figure 2A) and have a nearly zero $D^{17}\text{O}$, consistent with only mass-dependent fractionation affecting the ^{17}O content. This lack of correlation in seawater and higher $d^{18}\text{O}$ precipitation remains the same with a MDF coefficients of 0.521 (Figure S4). The high $d^{18}\text{O}$ extratropical precipitation samples are differentiated from the rest of the samples (by having negative values of $D^{17}\text{O}$) when a coefficient of 0.528 is used (Figure 1). These coefficient values (0.521 or 0.528) were derived from a regression of all data, including $d^{18}\text{O} > -4\text{‰}$ and, therefore, the selection of data used for estimating the MDF coefficient does not influence the lack of $D^{17}\text{O} - d^{18}\text{O}$ correlation in higher $d^{18}\text{O}$ waters.

The $D^{17}\text{O}$ magnitude of Antarctic surface snow from near the Terra Nova coast to Dome C (Figure 2B) increases nearly twofold (albeit as negative values), as does its tritium content (Figure S3). This observation supports the correlation of increasing $D^{17}\text{O}$ magnitude with greater stratospheric input because tritium is a proxy for stratosphere to troposphere mass transport (Lal and Peters, 1967; Fourre et al., 2006). The correlation of $D^{17}\text{O}$ with tritium has also been used to suggest a stratospheric influence on the ^{17}O of near-surface Antarctic snow (Winkler et al., 2013).

The increasingly negative values of $D^{17}\text{O}$ attributed to an increasing stratospheric input are counter-intuitive because stratospheric input has higher ^{17}O levels than tropospheric moisture. However, this is an artifact of the definition of $D^{17}\text{O}$ – relative to to $d^{18}\text{O}$ – and the very low $d^{18}\text{O}$ of stratospheric input. We can evaluate the impact of stratospheric ^{17}O input on tropospheric moisture $D^{17}\text{O}$ values using a two-component mixing model. Let f be the fraction of the stratospheric moisture component and r be the $d^{17}\text{O}/d^{18}\text{O}$ ratio in the stratospheric (st) or tropospheric (tr) fractions. Because tropospheric moisture would only have mass-dependent fractionation, r_{tr} is equivalent to l , the MDF coefficient. Then,

$$d^{18}\text{O}_{\text{mix}} = f d^{18}\text{O}_{st} + (1-f) d^{18}\text{O}_{tr} = f d^{18}\text{O}_{st} + d^{18}\text{O}_{tr} - f d^{18}\text{O}_{tr} \quad (4)$$

$$d^{17}\text{O}_{\text{mix}} = f d^{17}\text{O}_{st} + (1-f) d^{17}\text{O}_{tr} = f r_{st} d^{18}\text{O}_{st} + l d^{18}\text{O}_{tr} - f l d^{18}\text{O}_{tr} \quad (5)$$

and,

$$D^{17}\text{O}_{\text{mix}} = 1000 (d^{17}\text{O}_{\text{mix}} - l d^{18}\text{O}_{\text{mix}}) \quad (6)$$

Substituting (4) and (5) in (6) yields:

$$D^{17}\text{O}_{\text{mix}} = 1000 (f (r_{st} - l) d^{18}\text{O}_{st}) \quad (7)$$

Because the value of $d^{18}\text{O}_{st}$ would always be a negative number (Schmidt et al., 2005), Equation (7) shows that an increasing stratospheric fraction would result in $D^{17}\text{O}$ values that may be increasingly negative or positive depending upon r_{st} being greater than or less than l . An approximate value of r_{st} can be obtained from winter Antarctic precipitation when stratospheric input into the troposphere occurs by the Brewer-Dobson circulation (Pang et al., 2022; Winkler et al., 2013) and upper tropospheric air descends to low elevations near the ground surface (Roscoe, 2004). Regression of $d^{17}\text{O}$ versus $d^{18}\text{O}$ in winter Antarctic precipitation and surface snow (Landais et al., 2012; Touzeau et al., 2016) gives a r_{st} value of 0.530.

Thus, with a l value of 0.516 (or 0.521), less than the estimated r_{st} , $D^{17}\text{O}$ values would be negative and become more negative with an increasing stratospheric fraction. For l values greater than r_{st} (e.g., 0.534), $D^{17}\text{O}$ values would be positive. We observe the same patterns of $D^{17}\text{O} - d^{18}\text{O}$ correlations in tropical to polar precipitation (Figures 2 and S4). If the l value were to be closer to r_{st} , and may be higher or lower than r_{st} at different latitudes, the $D^{17}\text{O}$ values would be positive or negative and decrease or increase with decreasing $d^{18}\text{O}$. Such variable $D^{17}\text{O} - d^{18}\text{O}$ relationships are observed in tropical to polar precipitation with $l = 0.528$ (Figure 1).

3. The $D^{17}\text{O}$ Paleothermometer

The greater magnitudes of $D^{17}\text{O}$ in polar ice cores and the common correlation of $D^{17}\text{O}$ with $d^{18}\text{O}$ in polar and extratropical precipitation (Figure 2) support our hypothesis that $D^{17}\text{O}$ variations resulting from stratospheric ^{17}O input to the troposphere are conserved in precipitation. Thus, the $D^{17}\text{O}$ of precipitation may essentially be “fixed” once precipitation forms in the cloud. Any subsequent changes in precipitation $d^{17}\text{O}$ and $d^{18}\text{O}$ (by evaporation, diffusion etc) would occur by mass-dependent fractionation that would change the individual isotopic abundances but not $D^{17}\text{O}$ because the $D^{17}\text{O}$ of mass-dependent fractionation is zero (Thiemens, 2006). Further, the mass-dependent fractionation of ^{17}O relative to ^{18}O is *not* dependent on temperature (Angert et al., 2004). In other words, the behavior of $D^{17}\text{O}$ would be similar to that of a conservative tracer that is imparted to precipitation during its formation in the cloud, with the tracer concentration governed by condensation temperature, and subsequently remains unchanged in the water cycle. So instead of $d^{18}\text{O}$, $D^{17}\text{O}$ may provide a more robust and independent basis for reconstructing surface temperatures from ice core data. A $D^{17}\text{O}$ paleothermometer implies that the condensation temperatures are correlated with surface air temperature, an assumption that is commonly used in isotope paleothermometry (Petit et al., 1999; Buizert et al., 2021).

3.1. Calibration

We calibrated the $D^{17}\text{O}$ paleothermometer empirically by regression of $D^{17}\text{O}$ versus surface air temperatures in modern precipitation. Separate calibration data were used for Antarctica and Greenland because of the hemispherical asymmetry in stratospheric input (Rosenlof, 1995). Ideally, a reasonably large database of $D^{17}\text{O}$ in precipitation would be helpful for this calibration. But we only have a relatively small amount of data where both temperature and isotopic data are available. For Antarctica, precipitation data from Vostok and Dome C (Landais et al., 2012; Touzeau et al., 2016) were supplemented with data for surface snow from the Terra Nova coast to Dome C. This *de facto* combination of temporal and spatial isotope variations is compatible with our hypothesis for $D^{17}\text{O}$ variations. Data for summer months (November – February) was excluded so that precipitation would contain maximum stratospheric input and minimal mixing with lower tropospheric moisture (Baldwin et al., 2019). We were not able to find isotopic data for Greenland precipitation where temperature measurements also were reported. Therefore, we developed a calibration for the northern hemisphere by using extratropical precipitation data from southcentral USA (Indianapolis; Tian et al., 2019) and Europe (Madrid, Spain; Giménez et al., 2021) that partly overlap with the Greenland surface snow (Figure 2A). Only winter precipitation (December, January, February) data were used that were filtered to a $d^{18}\text{O}$ value less than -15% . These low $d^{18}\text{O}$ samples lie on or closest to the $D^{17}\text{O} - d^{18}\text{O}$ regression line for polar ice and snow (Figure 2). The temperature measurements for southcentral USA precipitation were reported from a nearby weather station and have a greater uncertainty. A statistical analysis of extratropical precipitation data identified two samples as outliers and these samples were excluded from the calibration dataset.

The $D^{17}\text{O}$ and temperature are well correlated ($R^2 = 0.69$ or 0.58) both for the southern and northern hemispheres (Figure 3) even though the calibration data are relatively small in numbers ($n=93$ and 44 , respectively). These correlations remain the same for a MDF coefficient value of 0.521 (Figure S5). The equations for the $D^{17}\text{O}$ paleothermometer ($l = 0.516$) are:

- a. Southern hemisphere (Antarctic): $D^{17}\text{O} = 9.93 T (^{\circ}\text{C}) - 91.6$
- b. Northern hemisphere: $D^{17}\text{O} = 6.42 T (^{\circ}\text{C}) - 168.2$

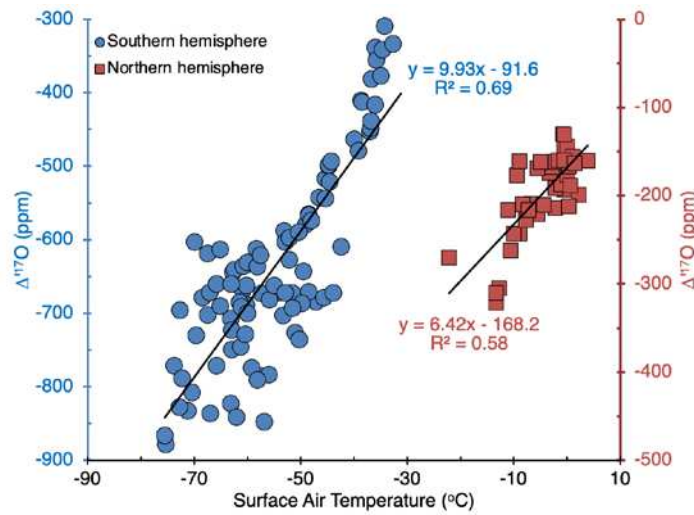
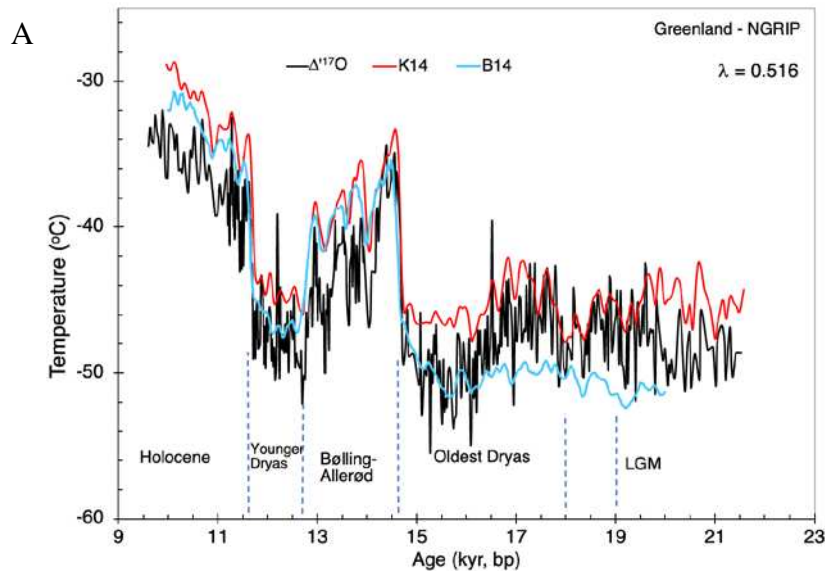
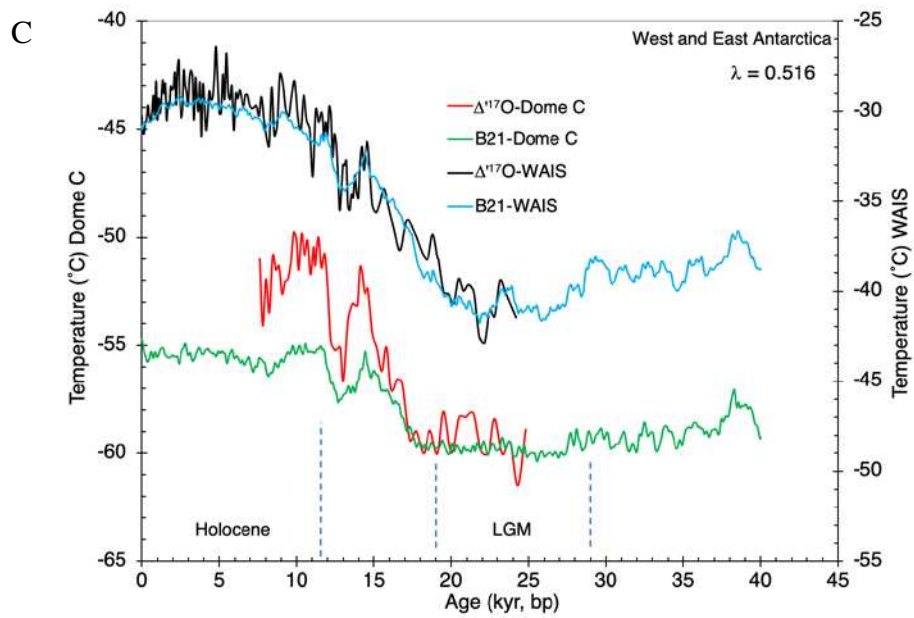
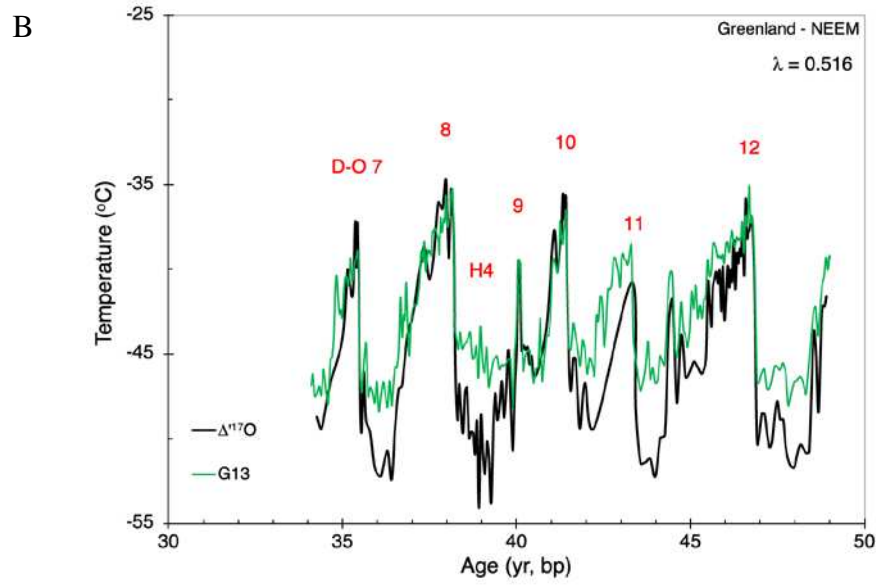


Figure 3. Calibration of the $D^{17}O$ paleothermometer. Southern hemisphere calibration used East Antarctic precipitation (Dome C, Vostok) and surface snow (traverse from the Terra Nova coast to Dome C). Northern hemisphere calibration used data for extratropical daily precipitation from southcentral USA and Spain. The p value for regression of each dataset is <0.001 .

A regression of estimated and measured temperatures for the two calibration datasets shows a strong correlation ($T_{\text{est.}} = 1.001 T_{\text{meas.}} - 0.097$; $R^2 = 0.92$). The standard error of this regression suggests an uncertainty of $\pm 7^\circ\text{C}$ for the $D^{17}O$ paleothermometer. This apparently large uncertainty reflects the small amount of data available for calibration. The actual uncertainty likely is much smaller as indicated by the similar magnitudes of temperature changes in different climates between our reconstruction and previous studies (Figure 4). The uncertainty from reported analytical error in $D^{17}O$ (± 10 ppm) is much smaller ($\pm 1.5^\circ\text{C}$) and subsumed within the larger statistical uncertainty.





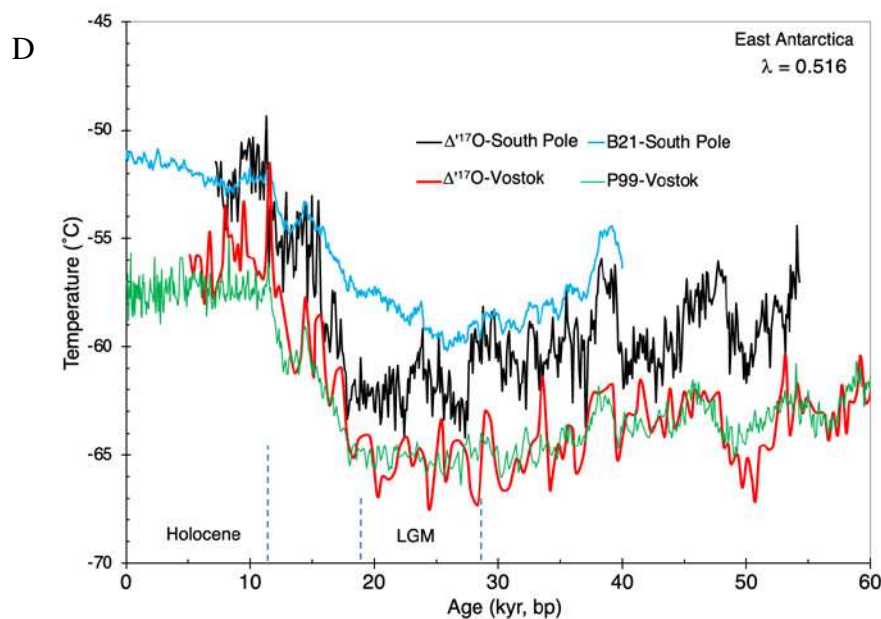


Figure 4. Reconstructed Greenland and Antarctic surface air temperatures. The age scales are GICC05 (Greenland) and AICC2012 (Antarctica). Dashed vertical lines show labeled climate periods. Estimated temperatures are labeled as follows: $D^{17}O$: this study; B14: from Buizert et al., 2014; K14: from Kindler et al., 2014; B21: from Buizert et al., 2021; G13: from Guillevic et al., 2013, after scaling to NGRIP reconstruction of Kindler et al., 2014; P99: from Petit et al., 1999, referenced to a present-day temperature of -57°C . Alpha-numeric labels in B refer to Dansgaard-Oeshger (D-O) or Heinrich (H) abrupt climate change events.

3.2. Temperature Reconstruction

Reconstructed surface air temperatures using ice core data from Greenland (NGRIP and NEEM), West Antarctica (WAIS) and East Antarctica (Dome C, South Pole, Vostok) are shown in Figure 4. The use of $D^{17}O$ overcomes the deficiencies in isotope paleothermometry based on $d^{18}O$ (Cuffey et al., 1995; Cuffey et al., 2016; Buizert et al., 2014). Specifically, the LGM to Holocene temperature rise in Greenland is about 16°C (Figure 4A), nearly twice that based on $d^{18}O$ but similar to that derived from borehole thermometry (Cuffey et al., 1995).

Similarly, our estimated temperature changes during abrupt climate change events (warming in the Bølling-Allerød interstadial, cooling in the Younger Dryas, or Dansgaard-Oeshger events 7 to 12) are $\sim 10^{\circ}\text{C}$ to 16°C (Figs. 4A, B). These estimates for abrupt events are much higher than those estimated by using $d^{18}O$ data, but are in excellent agreement with those estimated from gas phase analysis of air trapped in the ice (Severinghaus and Brook, 1999; Guillevic et al., 2013; Kindler et al., 2014). With an MDF coefficient of 0.521, estimated temperatures (Figure S6) are slightly warmer than those based on a coefficient value of 0.516 (Figure 4), but the magnitudes of warming from LGM to remain the same.

For the NGRIP ice core (Figure 4A), the same gas composition data but different firn densification models provide conflicting temperature estimates, particularly for ages older than about 15 kyr (Buizert et al., 2014; Kindler et al., 2014) (hereafter B14 and K14, respectively). A significant warming trend earlier than the onset of the Bølling-Allerød interstadial at 14.7 kyr is identified in B14, but not in K14, and estimated LGM temperatures at ~ 20 kyr are slightly colder ($\sim -51^{\circ}\text{C}$) in B14 than in K14 ($\sim -46^{\circ}\text{C}$). Our results show a warming trend beginning at ~ 15.7 kyr, in agreement with B14, but our LGM temperatures of $\sim -46^{\circ}\text{C}$ agree with K14, and with those estimated from borehole thermometry (Cuffey et al., 1995).

The temperatures determined using ice core data from NEEM (Figure 4B) also are in excellent agreement with those estimated in a previous study using gas phase analysis (Guillevic et al., 2013).

The original reconstruction of Guillevic et al., 2013 for NEEM was nearly the same as that for NGRIP, but the latter estimates have since been revised using different firn densification models (Kindler et al., 2014). This revision leads to NGRIP temperatures being warmer by ~ 4 °C. Therefore, we scaled the NEEM estimates of Guillevic et al. (2013) accordingly in Figure 4B. We can also estimate present day surface air temperature at NEEM using the $D^{17}O$ of shallow core samples of firn/snow for the years 2003–2005 (Landais et al., 2012). Our estimated temperature of about -26 °C compares with an estimate of -26.5 °C reconstructed using gas phase analysis (Orsi et al., 2017).

With data from Antarctic ice cores, our temperature reconstructions using the $D^{17}O$ paleothermometer (Figs. 4C, 4D) indicate an ~ 10 °C – 11 °C cooling during the LGM compared to the Holocene, both in the West (WAIS) and in the East (Dome C, South Pole, Vostok). Our results for West Antarctica (WAIS, Figure 4C) are in excellent agreement with those obtained using borehole thermometry (Cuffey et al., 2016) or by using both borehole and gas phase analysis (Buizert et al., 2021) (hereafter B21). But for East Antarctica, B21 suggested that the LGM cooling may have been only half ($\sim 4 - 7$ °C) of that in the West. This is inconsistent with our results which indicate similar degrees of cooling in West and East Antarctic. The discrepancy arises from East Antarctic reconstructions where B21 estimated a much earlier initiation of warming at South Pole (beginning at ~ 25 kyr), and relatively colder Holocene temperatures at Dome C, compared to our estimates. The earlier initiation of the South Pole warming trend is unlikely as it would initiate deglaciation within the LGM and is inconsistent with their own results for Dome C ice core (Figure 4C). The discrepancy between our results and B21 may also arise from a greater uncertainty in our limited dataset for calibration. However, we note that the slopes and intercepts for regression of Antarctic snow and extratropical precipitation datasets (Figs. 3, S5) are similar in spite of the hemispherical differences in stratospheric input. This similarity suggests that larger datasets may result in only minor revisions to the calibration used in this study. Alternatively, the discrepancy between our results and B21 may reflect a greater uncertainty in models of heat and gas diffusion and firn densification in regions of low snow accumulation (Jouzel et al., 2003) because our results are in excellent agreement with those of B21 for the high accumulation WAIS core site in West Antarctica (Figure 4C). Our results for the Vostok ice core in the low snow accumulation East Antarctic agree broadly with those based on spatial variations in d^2H (Petit et al., 1999). However, the extents of temperature change from LGM to Holocene or other longer-term climate changes are lower in d^2H based reconstructions (as is the case for estimates based on $d^{18}O$) compared to our results. A temperature reconstruction based on gas phase analysis was not available for the Vostok ice core.

4. Discussion

The magnitude of temperature changes (and of $D^{17}O$ because the relationship is linear) is greater in Greenland than Antarctica, both for the LGM to Holocene transition and for the abrupt climate change events (Figs. 4C, 4D, S6). These patterns are consistent with hemispherical differences in, and climate change impacts on, the stratospheric Brewer-Dobson Circulation. The mean age (or transit time from the tropics to the high latitudes) of stratospheric air reaching the troposphere is different in the two hemispheres owing to asymmetric planetary wave activity (Rosenlof, 1995). In the southern hemisphere, longer trajectories passing through higher altitudes result in a larger mean age. Longer residence times would facilitate greater isotope exchange of water vapor with NO_x species, which would lead to higher $d^{17}O$ values (Franz and Rockmann, 2005; Brinjikji and Lyons, 2021; Zahn et al., 2006). The *in situ* production of water by methane oxidation also increases with altitude within the stratosphere (Rosenlof, 1995). Thus, circulation trajectories at higher altitudes would further increase the $d^{17}O$ of stratospheric water vapor in the southern hemisphere than northern hemisphere. In addition, climate models suggest that during the LGM, tropical upwelling declined by about 12–17% relative to the present climate, leading to a weakened BDC and an increased mean age of stratospheric air in both hemispheres (Fu et al., 2020). Therefore, stratospheric air reaching the troposphere in the southern hemisphere would always carry a stronger MIF imprint, consistent with the greater magnitude of $D^{17}O$ in East Antarctica (Vostok, Dome C) compared to Greenland (Figure

2). In West Antarctica (WAIS), where the stratospheric input is diluted with a greater component of oceanic moisture (Stohl and Sodemann, 2010), $D^{17}\text{O}$ values are similar to those in Greenland (Figure 2). Because of the greater mean age of air in the southern hemisphere, the annual average mass cycled by the BDC is much less compared to that in the northern hemisphere (Rosenlof, 1995). More rapid cycling of mass in the northern hemisphere would result in a more rapid and larger change in $D^{17}\text{O}$ during abrupt climate change events over Greenland compared to Antarctica, which is consistent with observed differences (Figure 4; Figure S6).

The occurrence of abrupt climate change events in Greenland is attributed to abnormal heat transport to northern high latitudes by changes in the Atlantic meridional overturning circulation (AMOC) (He et al., 2022). However, the triggers of AMOC variability, including that from an increased freshwater forcing in the North Atlantic, remain a matter of debate (Capron et al., 2021). Changes in the strength of the stratospheric vortex may trigger multi-decadal perturbations in ocean circulation, which can account for a large portion of total AMOC variability (Reichler et al., 2012). Our results show a strong correlation between abrupt climate change and stratospheric input of ^{17}O owing to changes in BDC (Figure 4), supporting a stratospheric connection for AMOC variability.

Greenhouse gas-induced warmer climate is predicted to increase the tropical upwelling of tropospheric air and the BDC may increase by about 2–3% per decade (Baldwing et al., 2019). A faster BDC would lead to a lower mean age of stratospheric air and will impact the dynamics of stratosphere – troposphere interactions and weather on the earth's surface (Baldwin et al., 2019). Our results provide an observational constraint for climate models and a means to monitor the predicted impact of climate change on the BDC using the $D^{17}\text{O}$ of precipitation.

5. Conclusions

We have presented a revised analysis of precipitation ^{17}O by recognizing the separate effects of mass-dependent fractionation in the water cycle and stratospheric ^{17}O input to the troposphere. Contrary to existing interpretations, we concluded that while MDF is constant, stratospheric input is variable and causes of observed variability in precipitation ^{17}O . The stratospheric input is at a minimum in the tropics, where the net vertical mass flux is towards the stratosphere, and increases poleward. It reaches a maximum in Antarctica. We also concluded that the MDF coefficient for natural waters is about 0.516, which is less than the literature value of 0.528 because the literature value was derived from a dataset containing polar waters. Using a simple two-component mixing model, we demonstrated that a greater fraction of stratospheric air in the troposphere would result in increasingly more negative values of $D^{17}\text{O}$ as observed for polar samples. Our revised MDF coefficient value (0.516) is sufficient to explain the observed ^{17}O variability in all of the available published data on natural waters (precipitation, surface water, ice cores) from the tropics to the polar regions.

Based on this common correlation, it was possible to create a $D^{17}\text{O}$ paleothermometer calibrated with modern precipitation data. The past surface air temperatures based on $D^{17}\text{O}$ in many ice cores from Antarctica and Greenland were in excellent agreement with previous reconstructions based on borehole thermometry and on gas phase analysis of air trapped in ice. We concluded that the $D^{17}\text{O}$ approach overcame well-known deficiencies in temperature estimates that were based on $d^{18}\text{O}$ both for longer-term and abrupt climate changes.

The estimation of paleotemperatures turned out to be a simple application of a calibrated $D^{17}\text{O}$ – temperature relationship which is implemented without the use of complex models as is the case with borehole or gas phase analysis thermometry. Another important benefit of the $D^{17}\text{O}$ paleothermometer was that it did not require information on complex but poorly constrained processes that are known to affect temperature reconstructions based on precipitation $d^{18}\text{O}$. These processes include sea surface temperature and relative humidity at moisture origin, moisture transport, amount and seasonality of precipitation, changes in elevation at the site of precipitation, seawater $d^{18}\text{O}$, or post-depositional isotopic modification of surface snow. Because the $D^{17}\text{O}$ paleothermometer is based on the difference between the compositions of two isotopes, both of which

are proportionally affected by the processes noted above, our approach is more robust and independently applicable to a variety of climatic regimes. In addition to paleothermometry, precipitation $D^{17}O$ would be an obvious tool to monitor changes in stratosphere-troposphere mass exchange in response to greenhouse gas-induced climate change. Future availability of more extensive $D^{17}O$ datasets from precipitation in geographically diverse locations would contribute to a better understanding of stratosphere to troposphere mass-exchange and climate change impacts on the water cycle.

Supplementary Materials: The following supporting information can be downloaded at the website of this paper posted on Preprints.org.

Acknowledgments: We thank M. Guillevic, A. Landais, B. Stenni and R. Uemura for their kind assistance in providing electronic versions of some of their published isotope data; L. Wang for providing unpublished temperature measurements accompanying isotope data for Indianapolis, and J.W.C. White for assistance with locating web access to some of the Greenland isotope data.

Data Availability: Data used in this manuscript have been previously published and are available through references cited in the text.

References

- Aggarwal, P. K., U. Romatschke, L. Araguas-Araguas, D. Belachew, F. J. Longstaffe, P. Berg, C. Schumacher, A. Funk, Proportions of convective and stratiform precipitation revealed in water isotope ratios. *Nature Geosci.* 9, 624-629 (2016).
- Angert, A., Cappa, C. D., DePaolo, D. J. (2004) Kinetic ^{17}O effects in the hydrologic cycle: Indirect evidence and implications. *Geochim. Cosmochim. Acta*, 68, 3487-3495.
- Aron, P. G. et al. (2021) Variability and Controls on $\delta^{18}O$, d-excess, and $\Delta^{17}O$ in Southern Peruvian Precipitation. *J. Geophys. Res.: Atmospheres* 126, e2020JD034009. [Dataset] <https://agupubs.onlinelibrary.wiley.com/doi/abs/10.1029/2020JD034009>
- Aron, P. G., N. E. Levin, E. J. Beverly, T. E. Huth, B. H. Passey, E. M. Pelletier, et al. Triple oxygen isotopes in the water cycle. *Chem. Geol.* 565, 120026 (2021).
- Baldwin, M. P. et al. 100 years of progress in understanding the stratosphere and mesosphere. *Met. Monographs*, 59, 27-1 (2019).
- Baldwin, M. P., D. W. Thompson, E. F. Shuckburgh, W. A. Norton, N. P. Gillett (2003). Weather from the stratosphere? *Science*, 301, 317-319.
- Barkan E., B. Luz B. Diffusivity fractionations of $H_2^{16}O / H_2^{17}O$ and $H_2^{16}O / H_2^{18}O$ in air and their implications for isotope hydrology. *Rapid Comm. Mass Spectr.* 21, 2999–3005 (2007).
- Becagli, S. et al. (2004) Chemical and isotopic snow variability in East Antarctica along the 2001/02 ITASE traverse. *Annals Glaciol.* 39 473-482.
- Bhattacharya, S., M. Pal, B. Panda, M. Pradhan (2021). Spectroscopic investigation of hydrogen and triple-oxygen isotopes in atmospheric water vapor and precipitation during Indian monsoon season. *Isotopes Env. Health Studies*, 57 368-385. [Dataset] <https://www.tandfonline.com/doi/abs/10.1080/10256016.2021.1931169>
- Brinjkij, M., J. R. Lyons, Mass-independent fractionation of oxygen isotopes in the atmosphere. *Rev. Mineral. Geochem.* 86, 197-216 (2021).
- Buizert, C., Gkinis, V., Severinghaus, J. P., He, F., Lecavalier, B. S., Kindler, P., et al., Greenland temperature response to climate forcing during the last deglaciation. *Science*, 345, 1177-1180 (2014). [Dataset] <https://www.science.org/doi/abs/10.1126/science.1254961>
- Buizert, C., T. J. Fudge, W. H. Roberts, E. J. Steig, S. Sherriff-Tadano, C. Ritz, C., et al., Antarctic surface temperature and elevation during the Last Glacial Maximum. *Science*, 372, 1097-1101 (2021). [Dataset] <https://www.science.org/doi/abs/10.1126/science.abd2897>
- Capron, E., S. O. Rasmussen, T. J. Popp, T. Erhardt, H. Fischer, A. Landais, J. B. Pedro et al. The anatomy of past abrupt warmings recorded in Greenland ice. *Nature Comm.* 12, 1-12 (2021).
- Cuffey, K. M., Clow, G. D., Steig, E. J., Buizert, C., Fudge, T. J., Koutnik, M. et al., Deglacial temperature history of West Antarctica. *Proc. Natl. Acad. Sci.* 113, 14249-14254 (2016).
- Cuffey, K. M., G. D. Clow, R. B. Alley, M. Stuiver, M., E. D. Waddington, R. W. Saltus, Large arctic temperature change at the Wisconsin-Holocene glacial transition. *Science*, 270, 455-458 (1995).
- Dansgaard, W., S. J. Johnsen, H. B. Clausen, D. Dahl-Jensen, N. S. Gundestrup, C. U. Hammer, C. S. Hvidberg et al. Evidence for general instability of past climate from a 250-kyr ice-core record. *Nature* 364, 218-220 (1993).

- Fourré, E. et al Tritium records to trace stratospheric moisture inputs in Antarctica. *J. Geophys. Res.: Atmospheres*, 123, 3009–3018 (2018).
- Franz, P., T. Röckmann, High-precision isotope measurements of H₂¹⁶O, H₂¹⁷O, H₂¹⁸O, and the Δ¹⁷O-anomaly of water vapor in the southern lowermost stratosphere. *Atmos. Chem. Phys.* 5, 2949-2959 (2005).
- Fu, Q., R. H. White, M. Wang, B. Alexander, S. Solomon, A. Gettelman, D. S. Battisti, P. Lin. The Brewer-Dobson circulation during the last glacial maximum. *Geophys. Res. Lett.* 47, e2019GL086271 (2020).
- Garratt, J. R., M. Segal (1988) On the contribution of atmospheric moisture to dew formation. *Boundary-Layer Meteorol.* 45, 209-236.
- Giménez, R., M. Bartolomé, F. Gázquez, M. Iglesias, A. Moreno (2021) Underlying climate controls in triple oxygen (¹⁶O, ¹⁷O, ¹⁸O) and hydrogen (¹H, ²H) isotopes composition of rainfall (Central Pyrenees). *Frontiers Earth Sci.* 9, 633698. [Dataset] <https://www.frontiersin.org/articles/10.3389/feart.2021.633698/full#supplementary-material>
- Goering, M. A., W. A. Gallus Jr, M. A. Olsen, J. L. Stanford, Role of stratospheric air in a severe weather event: Analysis of potential vorticity and total ozone. *J. Geophys. Res. (Atmospheres)*, 106(D11), 11813-11823 (2001).
- Goursaud, S., V. Masson-Delmotte, V. Favier, S. Preunkert, M. Legrand, B. Minster, M. Werner. Challenges associated with the climatic interpretation of water stable isotope records from a highly resolved firn core from Adélie Land, coastal Antarctica. *The Cryosphere* 13, 1297-1324 (2019).
- Guillevic M., L. Bazin, A. Landais, P. Kindler, A. Orsi, V. Masson-Delmotte, T. Blunier, S. L. Buchardt, E. Capron, M. Leuenberger, P. Martinerie, F. Prié, B. M. Vinther, Spatial gradients of temperature, accumulation and δ¹⁸O-ice in Greenland over a series of Dansgaard-Oeschger events. *Clim. Past* 9, 1029–1051 (2013). [Dataset] <https://cp.copernicus.org/articles/9/1029/2013/>
- Guillevic, M. et al. (2013) Evidence for a three-phase sequence during Heinrich Stadial 4 using a multiproxy approach based on Greenland ice core records. *Clim. Past* 10 2115-2133.
- He, F., P. U. Clark, Freshwater forcing of the Atlantic meridional overturning circulation revisited. *Nature Clim. Change* 12, 449-454 (2022).
- He, S. et al. (2021) Understanding tropical convection through triple oxygen isotopes of precipitation from the Maritime Continent. *J. Geophys. Res.: Atmospheres* 126, e2020JD033418. [Dataset] : <https://agupubs.onlinelibrary.wiley.com/doi/full/10.1029/2020JD033418>
- Holton, J. R., P. H. Haynes, M. E. McIntyre, A. R. Douglas, R. B. Rood, L. Pfister, Stratosphere – troposphere exchange. *Rev. Geophys.* 33, 40– 439 (1995).
- Houze, R. A. jr., *Cloud Dynamics* (Elsevier, Oxford, UK, 2014).
- Johnsen, S. J., D. Dahl-Jensen, N. Gundestrup, J. P. Steffensen, H. B. Clausen, H. Miller, V. Masson-Delmotte, A. E. Sveinbjörnsdóttir, J. White. Oxygen isotope and palaeotemperature records from six Greenland ice-core stations: Camp Century, Dye-3, GRIP, GISP2, Renland and NorthGRIP. *J. Quat. Sci.* 16, 299-307 (2001).
- Jouzel, J., F. Vimeux, N. Caillon, G. Delaygue, G. Hoffmann, V. Masson-Delmotte, and F. Parrenin. Magnitude of isotope/temperature scaling for interpretation of central Antarctic ice cores. *J. Geophys. Res.: Atmospheres* 108, D12 (2003).
- Jouzel, J., R. B. Alley, K. M. Cuffey, W. Dansgaard, P. Grootes, G. Hoffmann, S. J. Johnsen et al. Validity of the temperature reconstruction from water isotopes in ice cores. *J. Geophys. Res.: Oceans.* 102, 26471-26487 (1997).
- Jouzel, Jean, Gilles Delaygue, Amaelle Landais, Valérie Masson-Delmotte, Camille Risi, and Françoise Vimeux. Water isotopes as tools to document oceanic sources of precipitation. *Water Resources Res.* 49, 7469-7486 (2013).
- Kaseke, K. F. et al. (2018) Precipitation origins and key drivers of precipitation isotope (¹⁸O, ²H, and ¹⁷O) compositions over Windhoek. *J. Geophys. Res.: Atmospheres* 123, 7311-7330. [Dataset] <https://agupubs.onlinelibrary.wiley.com/doi/10.1029/2018JD028470>
- Kindler P., Guillevic M., Baumgartner M., Schwander J., Landais A., Leuenberger M., Spahni R., Capron E., Chappellaz J., Temperature reconstruction from 10 to 120 kyr b2k from the NGRIP ice core. *Clim. Past* 10, 887–902 (2014). [Dataset] <https://cp.copernicus.org/articles/10/887/2014>
- Lal D., B. Peters, *Encyclopedia of Physics*, 46/2 (Springer-Verlag, Berlin, 1967).
- Landais, A. et al. (2012) Triple isotopic composition of oxygen in surface snow and water vapor at NEEM (Greenland). *Geochim. Cosmochim. Acta* 77, 304-316. [Dataset] <https://www.sciencedirect.com/science/article/abs/pii/S0016703711006740?via%3Dihub>
- Landais, A., A. Ekaykin, E. Barkan, R. Winkler, and B. Luz (2012) Seasonal variations of 17 O-excess and d-excess in snow precipitation at Vostok station, East Antarctica. *J. Glaciol.* 58, 725-733. [Dataset] <https://www.cambridge.org/core/journals/journal-of-glaciology/article/seasonal-variations-of-17-o-excess-and-d-excess-in-snow-precipitation-at-vostok-station-east-antarctica/F28723253C3A28D0E5C9A46FA58FABE9>

- Landais, A. et al. (2018) Ice core evidence for decoupling between midlatitude atmospheric water cycle and Greenland temperature during the last deglaciation. *Clim. Past* 14 1405-1415. [Dataset] <https://cp.copernicus.org/articles/14/1405/2018/>
- Landais, A., E. Barkan, B. Luz, Record of $\delta^{18}\text{O}$ and ^{17}O -excess in ice from Vostok Antarctica during the last 150,000 years. *Geophys. Res. Lett.* 35 (2008). [Dataset] <https://agupubs.onlinelibrary.wiley.com/doi/full/10.1029/2007GL032096>
- Landais, A., E. Barkan, D. Yakir, B. Luz, The triple isotopic composition of oxygen in leaf water. *Geochim. Cosmochim. Acta*, 70, 4105-4115 (2006).
- Landais, A., J. Lathiere, E. Barkan, and B. Luz. Reconsidering the change in global biosphere productivity between the Last Glacial Maximum and present day from the triple oxygen isotopic composition of air trapped in ice cores. *Global Biogeochem. Cycles* 21, (2007).
- Lin, Y., R. N. Clayton, L. Huang, N. Nakamura, J. R. Lyons, J. R. Oxygene isotope anomaly observed in water vapor from Alert, Canada and the implication for the stratosphere. *Proc. Natl. Acad. Sci.*, 110,15608-15613 (2013). [Dataset] <https://www.pnas.org/doi/full/10.1073/pnas.1313014110>
- Luz, B. E. Barkan, Variations of $^{17}\text{O}/^{16}\text{O}$ and $^{18}\text{O}/^{16}\text{O}$ in meteoric waters. *Geochim. Cosmochim. Acta*, 74, 6276-6286 (2010). [Dataset] <https://www.sciencedirect.com/science/article/abs/pii/S0016703710004643>
- Luz, B., E. Barkan, M. L. Bender, M. H. Thiemens, K. A. Boering (1999) Triple-isotope composition of atmospheric oxygen as a tracer of biosphere productivity. *Nature* 400, 547-550.
- Matejka, T. J., R. A. Houze Jr, P. V. Hobbs, Microphysics and dynamics of clouds associated with mesoscale rainbands in extratropical cyclones. *Quarterly J. Royal Met. Soc.* 106, 29-56 (1980).
- Meijer, H. A. J., W. J. Li (1998) The use of electrolysis for accurate $\delta^{17}\text{O}$ and $\delta^{18}\text{O}$ isotope measurements in water. *Isotopes Env. Health Studies* 34 349-369.
- Miller, M. F., Pack, A., Why measure ^{17}O ? Historical perspective, triple-isotope systematics and selected applications. *Rev. Min. Geochem.* 86, 1-34 (2021).
- Orsi, Anais J., et al. The recent warming trend in North Greenland. *Geophys. Res. Lett.* 44, 6235-6243 (2017).
- Pang, H. et al. (2019) Influence of summer sublimation on δD , $\delta^{18}\text{O}$, and $\delta^{17}\text{O}$ in precipitation, East Antarctica, and implications for climate reconstruction from ice cores. *J. Geophys. Res.: Atmospheres* 124, 7339-7358.
- Pang, H., P. Zhang, S. Wu, J. Jouzel, H. C. Christian Steen-Larsen, K. Liu, W. Zhang et al. The dominant role of Brewer–Dobson circulation on ^{17}O -excess variations in snow pits at Dome A, Antarctica. *J. Geophys. Res.: Atmospheres*: e2022JD036559 (2022).
- Petit, J., J. Jouzel, D. Raynaud, et al. Climate and atmospheric history of the past 420,000 years from the Vostok ice core, Antarctica. *Nature* 399, 429–436 (1999). [Dataset] <https://cdiac.ess-dive.lbl.gov/ftp/trends/temp/vostok/vostok.1999.temp.dat>
- Proposito, M. et al. (2002) Chemical and isotopic snow variability along the 1998 ITASE traverse from Terra Nova Bay to Dome C, East Antarctica. *Annals Glaciol.* 35, 187-194.
- Reichler, T., J. Kim, E. Manzini, J. Kröger, A stratospheric connection to Atlantic climate variability. *Nature Geosci.* 5, 783-787 (2012).
- Roscoe, H. K.: Possible descent across the “Tropopause” in Antarctic winter, *Adv. Space Res.*, 33, 7, 1048-1052 (2004).
- Rosenlof, K.H. Seasonal cycle of the residual mean meridional circulation in the stratosphere, *J. Geophys. Res.* 100 (D3), 5173–5191 (1995).
- Schmidt, G. A., G. Hoffmann, D. T. Shindell, Y. Hu. Modeling atmospheric stable water isotopes and the potential for constraining cloud processes and stratosphere-troposphere water exchange. *Journal of Geophysical Research: Atmospheres* 110, D21 (2005).
- Schmidt, Gavin A., Allegra N. LeGrande, and Georg Hoffmann. Water isotope expressions of intrinsic and forced variability in a coupled ocean-atmosphere model. *J. Geophys. Res: Atmospheres* 112, D10 (2007).
- Schoenemann, S. W. et al. (2014) Triple water-isotopologue record from WAIS Divide, Antarctica: Controls on glacial-interglacial changes in ^{17}O -excess of precipitation. *J. Geophys. Res.: Atmospheres* 119, 8741-8763. [Dataset] <https://agupubs.onlinelibrary.wiley.com/doi/full/10.1002/2014JD021770>
- Severinghaus J. P., Brook E. J., Abrupt climate change at the end of the last glacial period inferred from trapped air in polar Ice. *Science* 286, 930–934 (1999).
- Sharp, Z., J. A. G. Wostbrock, A. Pack, Mass-dependent triple oxygen isotope variations in terrestrial materials. *Geochem. Persp. Lett.* 7, 27-32 (2018).
- Sherwood, S. C., R. Roca, T. M. Weckwerth, N. G. Andronova, Tropospheric water vapor, convection, and climate. *Rev. Geophys.* 48, RG2001 (2009).
- Surma, J., Assonov, S., Herwartz, D., Voigt, C. and Staubwasser, M.: The evolution of ^{17}O -excess in surface water of the arid environment during recharge and evaporation, *Sci. Rep.*, 8, 4972, (2018).

- Steig, E. J., T. R. Jones, A. J. Schauer, E. C. Kahle, V. A. Morris, B. H. Vaughn, L. Davidge, J. W. C. White, Continuous-flow analysis of $\delta^{17}\text{O}$, $\delta^{18}\text{O}$ and δD of H_2O on an ice core from the South Pole. *Front. Earth Sci.* 9, 640292 (2021). [Dataset] <https://www.frontiersin.org/articles/10.3389/feart.2021.640292/full>
- Stohl, A., et al. (2003) Stratosphere – troposphere exchange: a review and what we have learned from STACCATO. *J. Geophys. Res.* 108(D12) 8516.
- Stohl, A., H. Sodemann, Characteristics of atmospheric transport into the Antarctic troposphere. *J. Geophys. Res.- Atmospheres*, 115(D2) (2010).
- Thiemens, M.H. History and applications of mass-independent isotope effects. *Annu. Rev. Earth Planet. Sci.* 34, 217-262 (2006).
- Thompson, D. W., & Solomon, S. (2002). Interpretation of recent Southern Hemisphere climate change. *Science*, 296(5569), 895-899.
- Tian, C., L. Wang, (2019) Stable isotope variations of daily precipitation from 2014–2018 in the central United States. *Sci. Data*, 6, 1-8. [Dataset] <https://www.nature.com/articles/s41598-018-25102-7#Sec20>
- Touzeau, A. et al. (2016) Acquisition of isotopic composition for surface snow in East Antarctica and the links to climatic parameters. *The Cryosphere* 10, 837-852. [Dataset] <https://hal-insu.archives-ouvertes.fr/insu-01388903>
- Uechi, Y., R. Uemura (2019) Dominant influence of the humidity in the moisture source region on the ^{17}O -excess in precipitation on a subtropical island. *Earth Planet. Sci. Lett.* 513 20-28. [Dataset] : <https://www.sciencedirect.com/science/article/abs/pii/S0012821X19301098>
- Uemura, R., E. Barkan, O. Abe, B. Luz, Triple isotope composition of oxygen in atmospheric water vapor, *Geophys. Res. Lett.* 37, L04402 (2010).
- Voigt, C., D. Herwartz, C. Dorador, M. Staubwasser (2021) Triple oxygen isotope systematics of evaporation and mixing processes in a dynamic desert lake system. *Hydrol. Earth System Sci.* 25, 1211-1228. [Dataset] : <https://hess.copernicus.org/articles/25/1211/2021/>
- Winkler, R., A. Landais, C. Risi, M. Baroni, A. Elaykin, J. Jouzel, J.R. Petit, F. Prie, B. Minster, S. Falourd, Interannual variation of water isotopologues at Vostok indicates a contribution from stratospheric water vapor. *Proc. Natl. Acad. Sci.* 110, 17674-17679 (2013). [Dataset] : <https://cp.copernicus.org/articles/8/1/2012/>
- Winkler, R., et al. (2012) Deglaciation records of ^{17}O -excess in East Antarctica: reliable reconstruction of oceanic normalized relative humidity from coastal sites. *Clim. Past* 8, 1-16.
- Zahn, A., P. Franz, C. Bechtel, J-U. Grooß, T. Röckmann. Modelling the budget of middle atmospheric water vapour isotopes. *Atmos. Chem. Phys.* 6, 2073-2090 (2006)

Disclaimer/Publisher's Note: The statements, opinions and data contained in all publications are solely those of the individual author(s) and contributor(s) and not of MDPI and/or the editor(s). MDPI and/or the editor(s) disclaim responsibility for any injury to people or property resulting from any ideas, methods, instructions or products referred to in the content.